



This provides four quadrant power controllability to multilevel current source HVDC transmission and, thus, makes this alternative equally flexible to PWM controlled voltage source conversion, without the latter's limitations in terms of power and voltage ratings. It has been shown theoretically and verified by MATLAB/Simulink simulation and results describe its effectiveness.

### III. PROPOSED SYSTEM

SHE-PWM for Harmonic immunity in VSC-HVDC Transmission using PV energy system. The project discusses optimized modulation patterns which offer controlled harmonic immunity between the ac and dc side. The application focuses on the conventional two-level converter when its dc-link voltage contains a mix of low-frequency harmonic components. Simulation results are presented to confirm the validity of the proposed switching patterns. A general idea of the modern progress of VSC based HVDC technologies is accessible. The mainly important organize and methods of modeling HVDC with VSC modules and the directory of presented installations also exist. The primary production of power utility converters is depending on topologies of current-source converter (CSC). Nowadays, lots of projects yet use the CSCs owing to their ultra-high capabilities of power. With the discovery of completely restricted power semiconductors, such as IGBTs and IGCTs-integrated gate-commutated thyristors, the topologies of VSC are further striking owing to their characteristics of four-quadrant power-flow. A distinctive pattern of the HVDC power transmission system with VSC is publicized in Figure.1 as it is publicized.

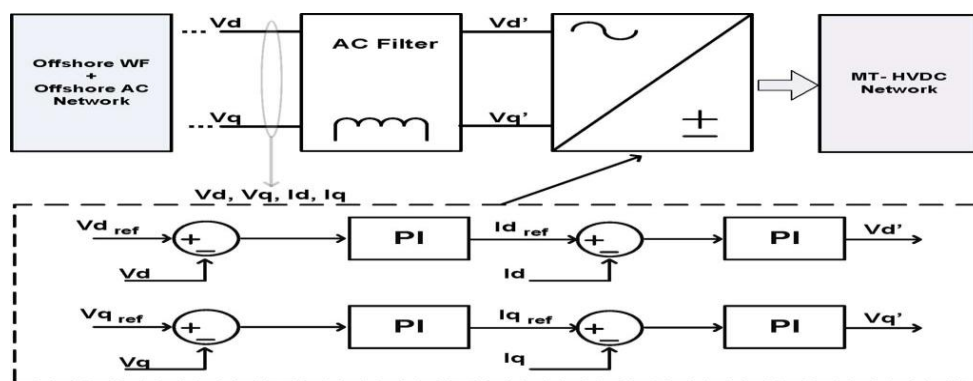


Fig.2 Phase of the two-level VSC for the HVDC power transmission system

The topologies of multilevel for high-power, high-voltage VSCs are as well in brief conversed. Multi-level converters may be further proficient but they are less dependable owing to the superior number of mechanism and the difficulty of their managing and creation. Raising the integer of levels over three is a hard mission for the production. Though, variations at different frequencies frequently happen on the dc area which usually emerges as harmonics of the ac-side working frequency. The mainly important harmonic established to the spectrum of dc voltage by an unstable 3-phase ac-network is the second harmonic. Inverters having second harmonic on the bus of dc produce the 3<sup>rd</sup> harmonic on ac side. The exclusion of inverter harmonics of lower-order with variable voltage as input is illustrated.

#### A. OFFSHORE AC GRID VOLTAGE CONTROL

The projected M-type intonation method permits 33% of decline in the switching transitions lacking lowering the sort of the chief harmonic. The algebraically method proposes an arithmetical computation by adjusting the Pulse width to terminate the harmonics created by the voltage of dc ripple. It has lesser total harmonic distortion (THD) while compared with the conservative triangular sine PWM in the case wherever the dc voltage also oscillates. However sinusoidal-PWM techniques, which need a comparatively elevated number of transitions for each cycle to remove the low-range harmonics. SHE-

PWM is the harmonic control with the lowest probable operation to give firmly restricted spectrum of voltage and increases the bandwidth among the essential frequency and the first important harmonic.

In case of a fault, healthy converters (connected to non-faulted ac mainland grids) are not able to increase their power injection and power dissipation in chopper resistors is required in order to mitigate the dc voltage rise. Based on this assumption, each dc chopper must be sized to dissipate the nominal power of the HVDC–VSC to which it is connected. The dc chopper de-activation occurs if:

- 1) The dc voltage reaches a value below the threshold activation level (eg. after fault clearance) or;
- 2) The chopper resistor temperature overreaches the maximum value (thermal protection tripping), meaning that the resistor maximum energy dissipation capability has been overreached.

This specific situation is often related to a permanent fault event and must be handle by additional control schemes to perform permanent active power reduction at offshore WF-level.

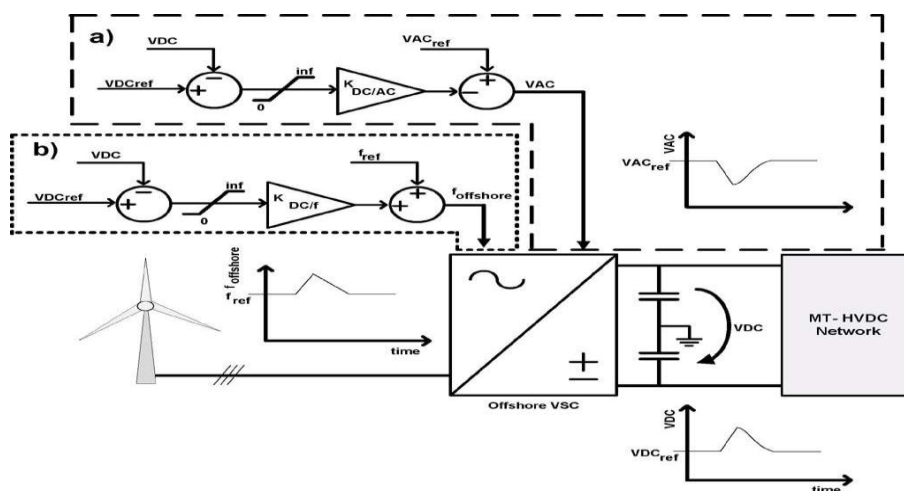


Fig3. Control scheme for FRT provision based on dc voltage (a) AC offshore grid voltage control. (b) AC offshore grid frequency control.

#### IV. PHOTOVOLTAIC SYSTEM

Grid connected photovoltaic (PV) power conversion systems are getting more and more attention in the last decade, mainly due to cost reduction of PV modules and government incentives, which has made this energy source and technology competitive among other energy sources. Photovoltaics’ is the field of technology and research related to the devices which directly convert sunlight into electricity using semiconductors that exhibit the photovoltaic effect. Photovoltaic effect involves the creation of voltage in a material upon exposure to electromagnetic radiation.

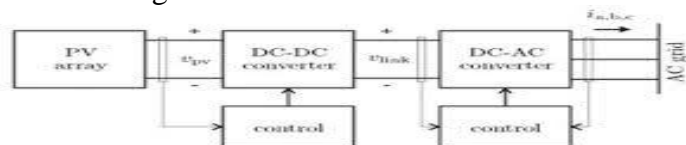


Figure 1: Block diagram of the PV system. Fig: 4 PV systems for proposed technique

##### A. SELECTIVE HARMONIC ELIMINATION

Note that in the SPWM scheme developed over, a great amount of switching is needed, through the consequential connected losses of switching. By means of the process of Selective Harmonic Elimination, simply certain harmonics are eradicated with the least number of switching. This process though can be complicated for implementing on-line owing to calculation and memory needs. For a PWM waveform with two levels having odd plus half wave symmetries with n chops for each cycle of quarter as given in Fig,

the magnitude peak of the harmonic components together with the fundamental, are specified by equation(1). In this case  $h_i$  is the  $i$ th harmonic magnitude and  $\alpha_j$  is the angle of  $j$ th primary switching. Still harmonics do not see up since of the symmetry of half-wave. These  $n$  chops of waveform give  $n$  degrees of choice. Numerous controlling options are thus probable. For instance,  $n$  certain harmonics can be removed. An additional choice that is used here is for eliminating  $n-1$  certain harmonics and uses remain degree of choice for controlling the ac voltage of fundamental frequency. To discover the mandatory to attain this purpose, it is enough to set the equivalent  $h$ 's in the given equations to the required values and resolve for the  $\alpha_j$  s.

$$\begin{aligned}
 h_1 &= \left(4 \cdot \frac{E}{\pi}\right) \cdot [1 - 2 \cos \alpha_1 + 2 \cos \alpha_2 - 2 \cos \alpha_3 \dots 2 \cos \alpha_n] \\
 h_3 &= \left(4 \cdot \frac{E}{3\pi}\right) \cdot [1 - 2 \cos 3 \alpha_1 + 2 \cos 3 \alpha_2 - 2 \cos 3 \alpha_3 \dots 2 \cos 3 \alpha_n] \\
 h_k &= \left(4 \cdot \frac{E}{k\pi}\right) \cdot [1 - 2 \cos k \alpha_1 + 2 \cos k \alpha_2 - 2 \cos k \alpha_3 \dots 2 \cos k \alpha_n] \dots \dots \dots (1)
 \end{aligned}$$

Equation (1) can be gladly verified by finding the waveform Fourier coefficients shown in figure. Normally, for a cyclic waveform with period  $2\pi$ , the Fourier Sine and Cosine Coefficients are specified with:

$$\begin{aligned}
 a_o &= \frac{1}{2\pi} \int_0^{2\pi} f(\theta) d\theta \\
 a_o &= \frac{1}{\pi} \int_0^{2\pi} f(k\theta) \cos(k\theta) d\theta \\
 b_k &= \frac{1}{\pi} \int_0^{2\pi} f(k\theta) \sin(k\theta) d\theta \\
 b_k &= \frac{4}{\pi} \int_0^{2\pi} f(k\theta) \sin(k\theta) d\theta \dots \dots \dots (2)
 \end{aligned}$$

Since the symmetry waveform of the half-cycle is simply harmonics of odd order exist. As well, it is simple to observe that the Cosine Fourier coefficients vanish with the option of coordinate axes used. Using the symmetry of quarter cycle, the Sine Fourier coefficients become:

$$\begin{aligned}
 b_n &= \frac{4E}{\pi} \left( \int_0^{\alpha_1} \sin(k\theta) d\theta - \int_{\alpha_1}^{\alpha_2} \sin(k\theta) d\theta - \int_{\alpha_2}^{\alpha_3} \sin(nk) d\theta \dots \int_{\alpha_n}^{\frac{\pi}{2}} \sin(k\theta) d\theta \right) \\
 &= \frac{4E}{\pi K} \left( -\cos(k\theta) \Big|_0^{\alpha_1} + \cos(k\theta) \Big|_{\alpha_1}^{\alpha_2} - \cos(k\theta) \Big|_{\alpha_2}^{\alpha_3} \dots \right) \\
 &= \frac{4E}{\pi K} (1 - 2 \cos n \alpha_1 + 2 \cos k \alpha_2 - 2 \cos k \alpha_3 \dots 2 \cos k \alpha_n) \dots \dots \dots (3)
 \end{aligned}$$

### V. SIMULATION RESULTS

The MATLAB software is used to demonstrate the dc-link ripple-voltage repositioning technique. Key results are presented in Fig5. The two-terminal system, it is still possible to transfer power in case the DC slack converter fails or blocks. Figure shows simulation results for the voltage margin control implemented in the 4-terminal VSC HVDC system using MATLAB/Simulink. The power flow has been initialized such that the average voltage is equal to unity.

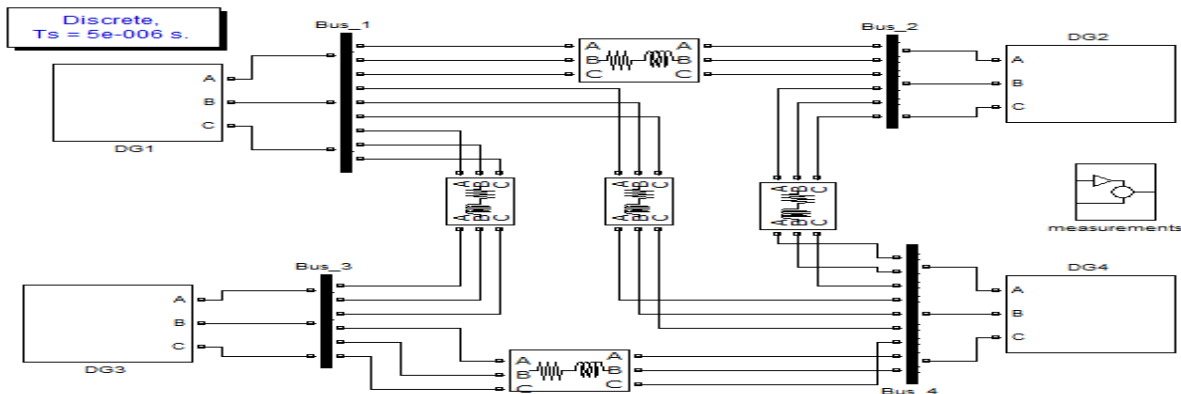


Fig5: SHE-PWM for Harmonic immunity in VSC-HVDC Transmission using PV system

After the outage of the DC voltage controlling converter 2, converter 3 initially tries to control the converter voltage when its converter upper voltage limit is reached. Since its current limit is hit, converter 3 is unable to control the converter voltage further, resulting in a further increase of the DC system voltage, after which converter 1 takes over the voltage control. The power in converter 4 remains unchanged because the influence of the changing DC voltage is not fed back to the power controlling converters as long as the voltage limits are not hit.

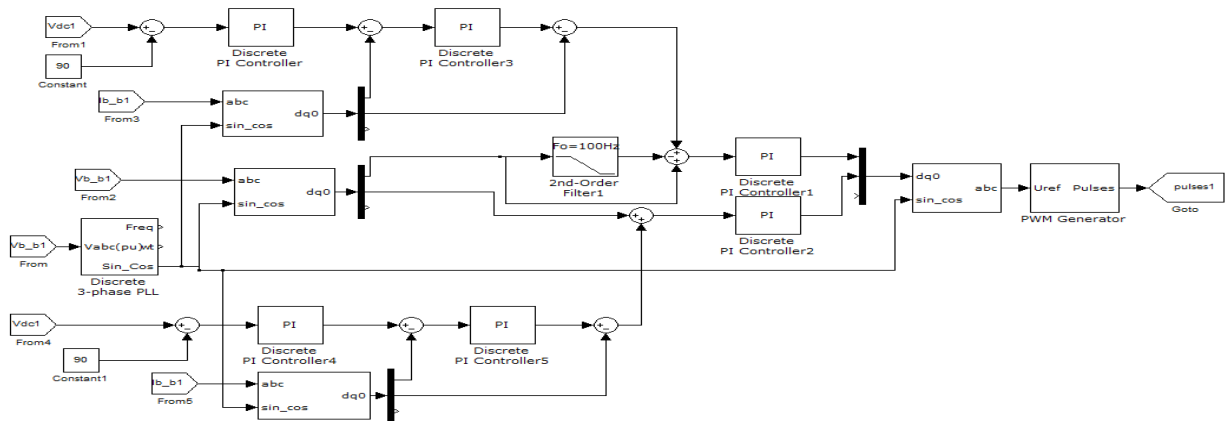


Fig6: Simulink circuit for SRF theory

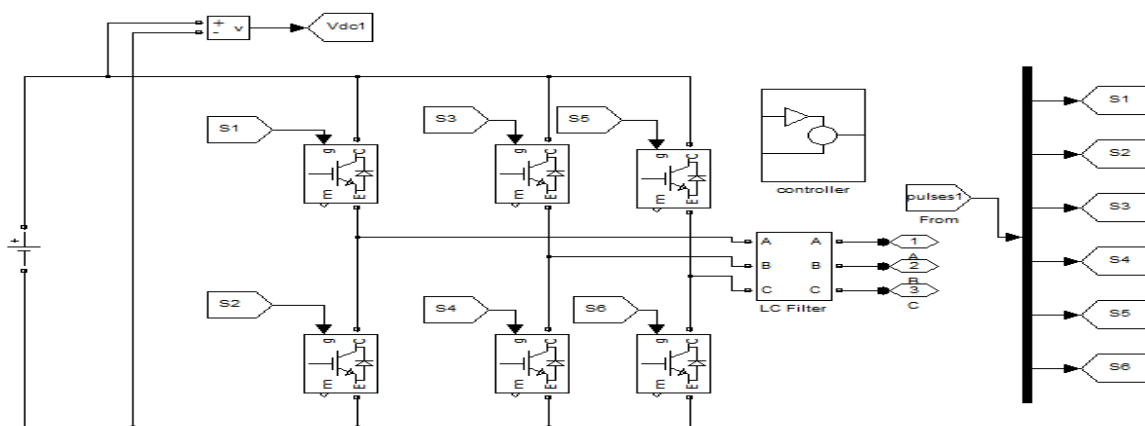


Fig7: Simulink circuit for Three-phase two-level VSC inverter

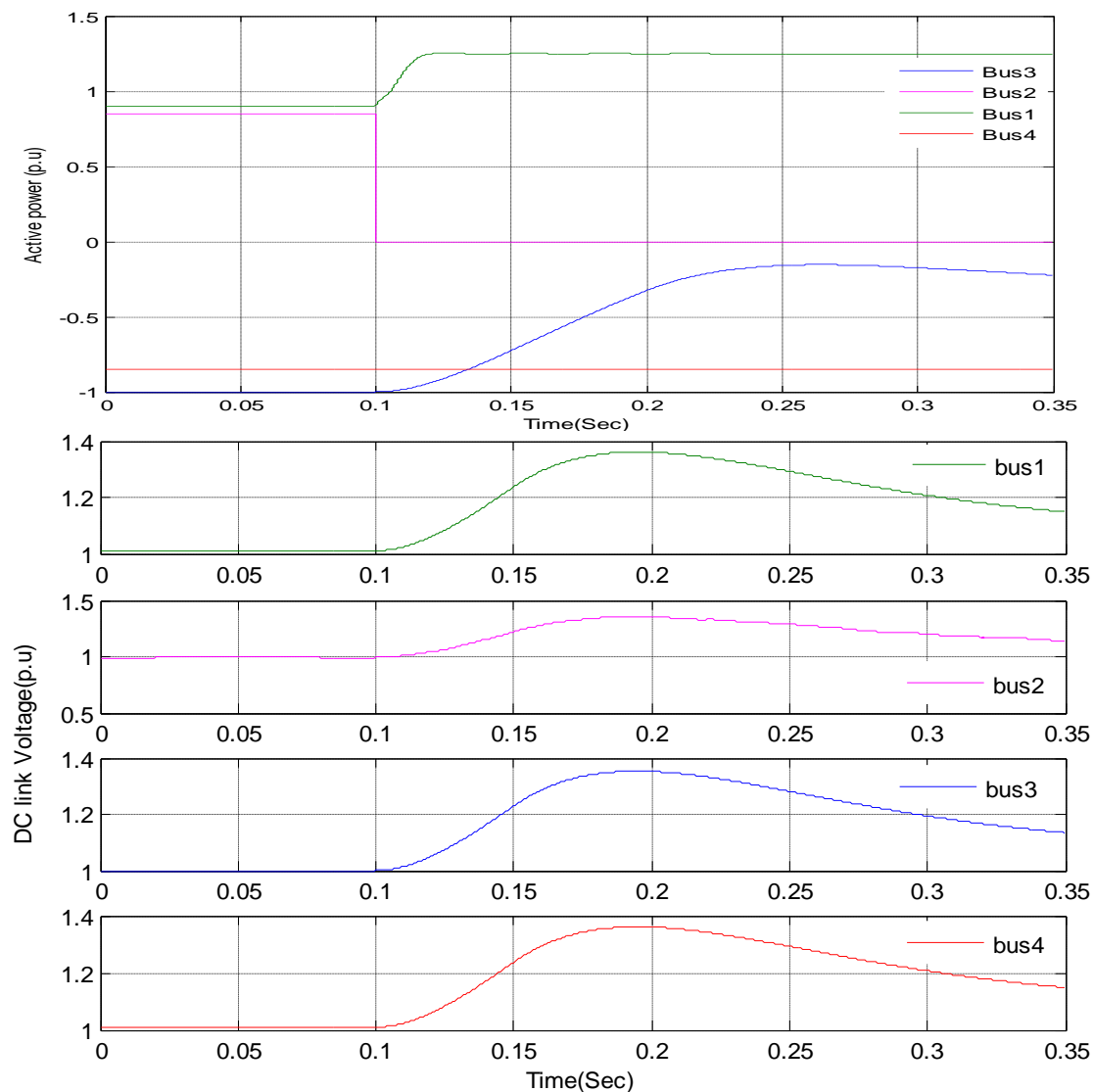


Fig8: Interactions of converters in the DC grid after outage of converter 2: (a) Active power to the AC grid and (b) DC voltage

A 20% active power step at  $t = 0.1$  s, and a 100% active power step at  $t = 0.1$  s is simulated. The simulation has been performed for three different models: the model with voltage limit included, the model with voltage limit neglected, and the model with simplified current controller. In Fig. 8, a close up around  $t = 0.1$  s is shown. For the 20% step, the results of the three models correspond well. In Fig. 9, a close up around  $t = 0.1$  s is shown. For this larger step, it can be clearly seen that the dynamic behavior of the model with voltage limit is different. The rise time is slower and the maximum value of power in the first swing is higher (73 MW versus 55 MW). This is not captured in the simplified model. The lower graph shows the voltage, which is limited at 1.05 p.u. for the model with limit. The full simulation is shown in Fig8. It is left to the appreciation of the reader if and in which situation neglecting the voltage limit is acceptable.

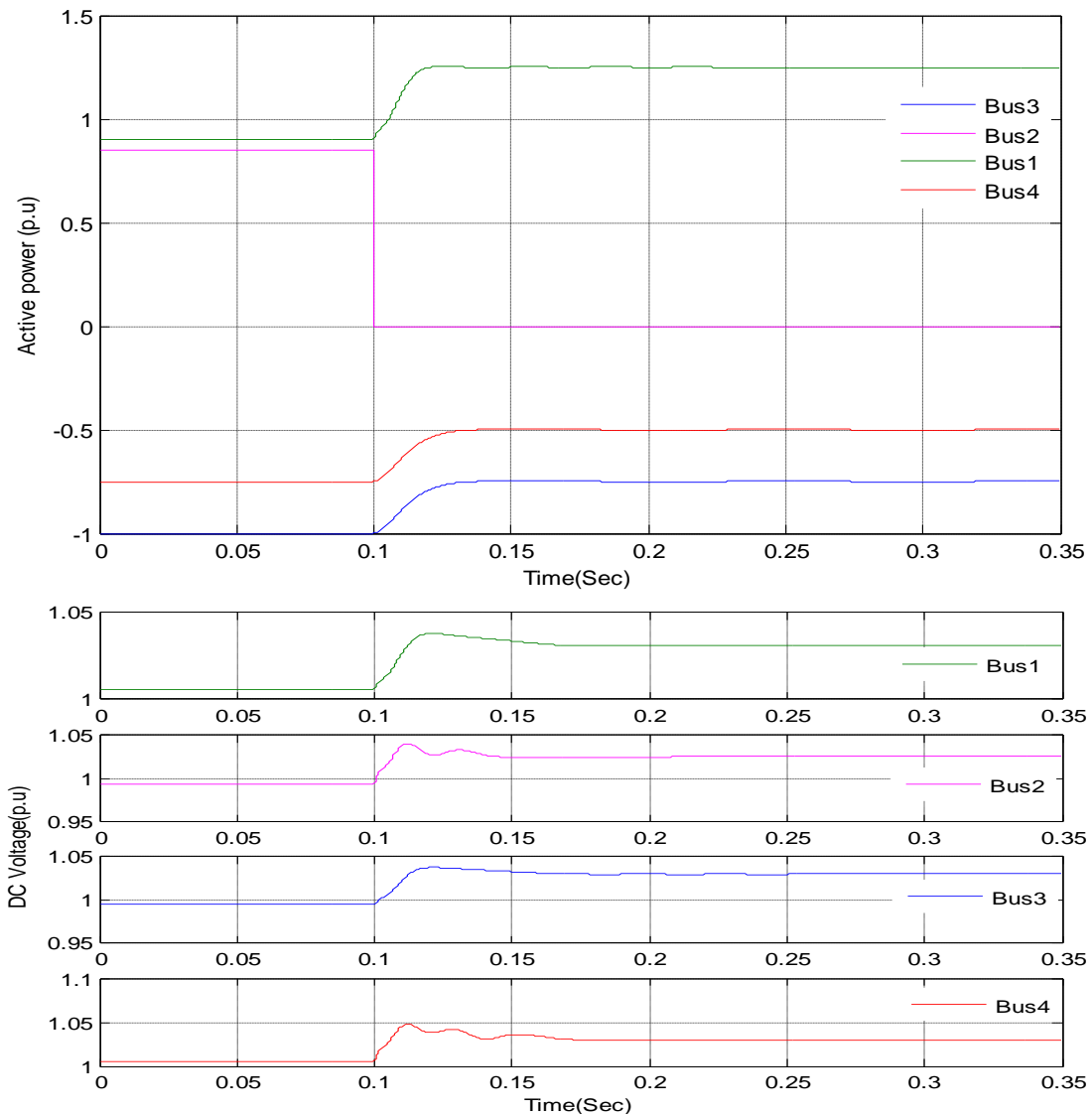


Fig9: Interactions of converters in the DC grid after outage of converter 2 (Voltage droop control): (a) Active power to the AC grid and (b) DC voltage

In the simulations, the control scheme continues operating as a voltage droop scheme, since no voltage limits were hit at any of the converters. Similarly, to the results in case of the voltage margin control in Fig.9, converter 1 hits a current limit, which is accounted for by the other converter's droop action. The advantage of this voltage droop over the voltage margin control, is that the power after the converter outage is shared amongst the different droop controlled converters in the DC system, which makes the voltage droop control a suitable candidate for an operation in large DC grids.

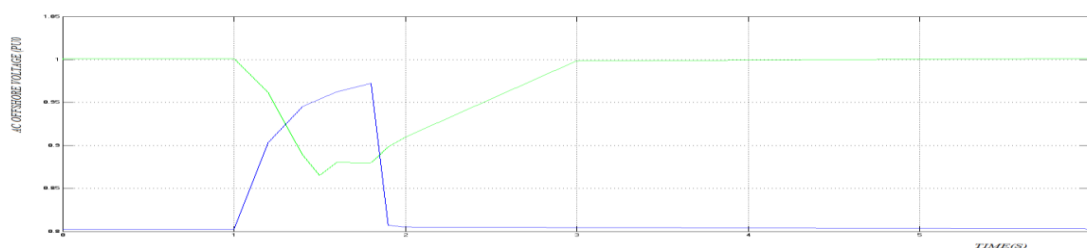


Fig10: Regulated frequency and voltage at off-shore HVDC-VSC station

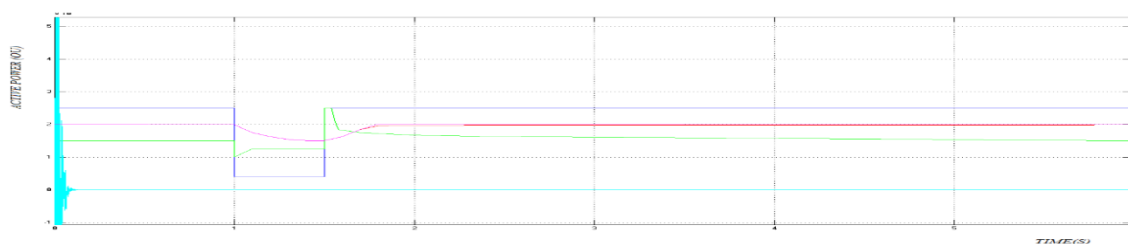


Fig11: DC-grid voltage profile and power flow at HVDC-VSC (case a).

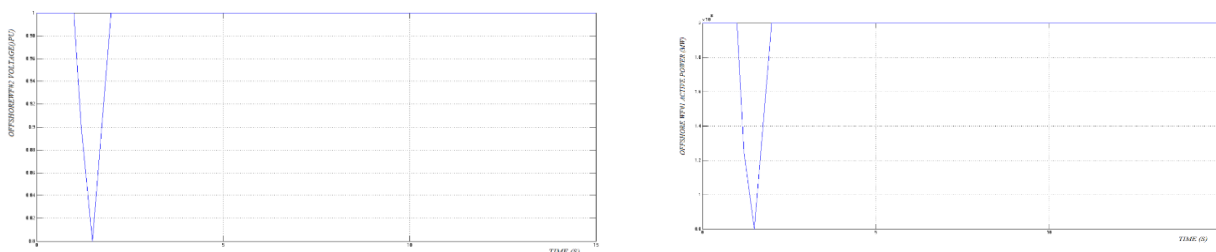


Fig12. MTDC grid voltage profile and PMSG-based WF response with respect to the variation of the droop

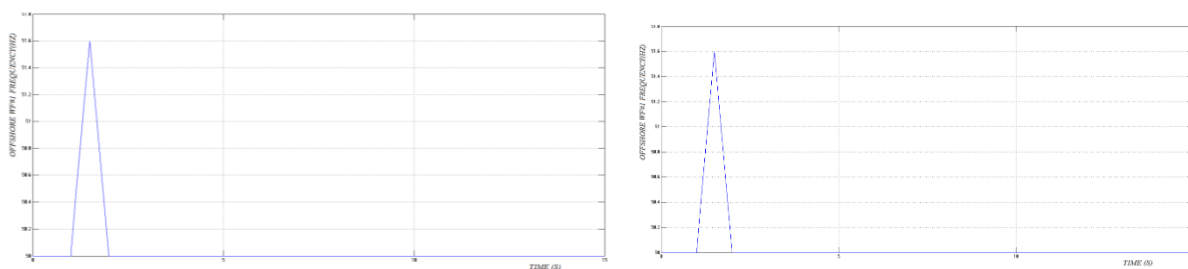


Fig13. Impact of the frequency control time delay in the DFIG-based WF

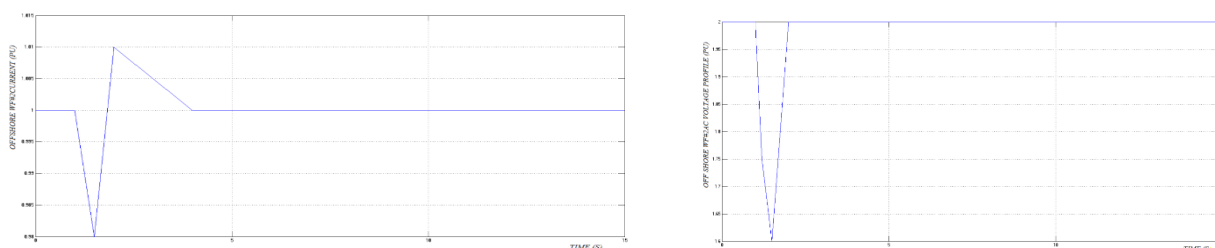


Fig.14 shows the simulation results of the method for the case that the dc-bus voltage has no ripple.

The modulating signal is equal to the modulation index since the dc-link voltage is constant. Hence, the results are identical to the ones taken by using conventional SHE-PWM with a fixed modulation index (i.e., 0.75). Fig11. shows what happens when 10% of 2nd harmonic is added to the dc-link voltage. The switching angles are unchanged but the amplitude of the output voltage is fluctuating. The modulating signal is forced to be constant to give the same results with the conventional SHE-PWM. The value of the fundamental component is increased by 5% and a value of the 3rd harmonic is equal to 5% of the fundamental that appears in the spectrum of Figure13. By applying the dc-link ripple-voltage repositioning (Fig. 8), it is observed that the switching angles have slightly shifted.

## VI. CONCLUSION

This paper provides a discussion on the identification and development of communication-free control strategies for FRT provision on MTDC grids interconnecting offshore WF with ac mainland grids. The proposed control strategies for endowing MTDC grids with FRT capability share a common characteristic: the accommodation/dissipation of active power from off-shore WF in order to mitigate the dc voltage rise effect.

The major advantage of these strategies relies on less investment regarding the implementation of the required control functionalities. However, these strategies lead to some stress over DFIGN in terms of speed variations (similarly to what happens in wind turbines connected to onshore grids). Also, small over currents are observed in the associated HVDC-VSC and must be considered in the design phase. This is an online method which can be applied for eliminating any low-order harmonic frequency regardless of amplitude or phase shift of the ripple. There are some limitations related to the maximum modulation index available for SHE-PWM angles. The repositioning technique also causes a reflection with respect to the midpoint between the fundamental component and the first significant harmonic. There are cases where the technique is not beneficial. On the other hand, it eliminates all low-order ac-side harmonics for every dc-bus ripple voltage of frequency below the midpoint harmonic.

## REFERENCES

- [1] European Union Project TWENTIES. [Online]. Available: <http://www.twenties-project.eu> Oct. 2012
- [2] K. Bell, D. Cirio, A. M. Denis, L. He, C. C. Liu, G. Migliavacca, C. Moreira, and P. Panciatici, "Economic and technical criteria for de-signing future off-shore HVDC grids," in *Proc. Power Energy Soc. In-novative Smart Grid Technol. Conf. Eur.*, 2010, pp. 1–8.
- [3] Intelligent Energy Europe. OffshoreGrid Project, 2012. [Online]. Avail-able: <http://www.offshoregrid.eu/>
- [4] Intelligent Energy Europe. Tradewind Project, 2012. [Online]. Avail-able: <http://www.trade-wind.eu>
- [5] T. Ackermann, "Transmission systems for offshore wind farms," *IEEE Power Eng. Rev.*, vol. 22, no. 12, pp. 23–27, Dec. 2002.
- [6] N. B. Negra, J. Todorovic, and T. Ackermann, "Loss evaluation of HVAC and HVDC transmission solutions for large offshore wind farms," *Elect. Power Syst. Res.*, vol. 76, no. 11, pp. 916–927, 2006
- [7] N. Flourentzou, V. G. Agelidis, and G. D. Demetriades, "VSC-based HVDC power transmission systems: An overview," *IEEE Trans. Power Electron.*, vol. 24, no. 3, pp. 592–602, Mar. 2009.
- [8] O. Gomis-Bellmunt, J. Liang, J. Ekanayake, R. King, and N. Jenkins, "Topologies of multiterminal HVDC-VSC transmission for large off-shore wind farms," *Elect. Power Syst. Res.*, vol. 81, no. 2, pp. 271–281, 2011.
- [9] O. Gomis-Bellmunt, J. Liang, J. Ekanayake, and N. Jenkins, "Voltage—current characteristics of multiterminal HVDC-VSC for offshore wind farms," *Elect. Power Syst. Res.*, vol. 81, no. 2, pp. 440–450, 2011.
- [10] S. Cole, J. Beerten, and R. Belmans, "Generalized dynamic VSC MTDC model for power system stability studies," *IEEE Trans. Power Syst.*, vol. 25, no. 3, pp. 1655–1662, Aug. 2010.
- [11] B. Silva, C. L. Moreira, L. Seca, Y. Phulpin, and J. A. P. Lopes, "Pro-vision of inertial and primary frequency control services using offshore multiterminal HVDC networks," *IEEE Trans. Sustain. Energy*, vol. 3, no. 4, pp. 800–808, Oct. 2012.
- [12] M. Tsili and S. Papathanassiou, "A review of grid code technical re-quirements for wind farms," *IET Renew. Power Gen.*, vol. 3, no. 3, pp. 308–332, 2009.
- [13] F. D. Bianchi, O. Gomis-Bellmunt, A. Egea-Alvarez, and A. Junyent-Ferre, "Optimal control of voltage source converters for fault operation," in *Proc. 14th Eur. Power Electron. Appl. Conf.*, Aug. 30–Sep. 1, 2011, p. 1, 10.
- [14] T. D. Vrionis, X. I. Koutiva, N. A. Vovos, and G. B. Giannakopoulos, "Control of an HVDC link connecting a wind farm to the grid for fault ride-through enhancement," *IEEE Trans. Power Syst.*, vol. 22, no. 4, pp. 2039–2047, Nov. 2007.
- [15] C. Feltes, H. Wrede, F. W. Koch, and I. Erlich, "Enhanced fault ride-through method for wind farms connected to the grid through VSC-based HVDC transmission," *IEEE Trans. Power Syst.*, vol. 24, no. 3, pp. 1537–1546, Aug. 2009.
- [16] G. Ramtharan, A. Arulampalam, J. B. Ekanayake, F. M. Hughes, and N. Jenkins, "Fault ride through of fully rated converter wind turbines with AC and DC transmission," *IET Renew. Power Gen.*, vol. 3, no. 4, pp. 426–438, 2009.
- [17] L. Xu and L. Yao, "DC voltage control and power dispatch of a multi-terminal HVDC system for integrating large offshore wind farms," *IET Renew. Power Gen.*, vol. 5, no. 3, pp. 223–233, 2011.
- [18] J. McDonald, "Leader or follower [The business scene]," *IEEE Power Energy Mag.*, vol. 6, no. 6, pp. 18–90, Nov. 2008.



<sup>1</sup>Meesala Nareshhe has completed his B.TECH Electrical & Electronics Engineering in BVCECodalarevu Amalapuram and is currently pursuing his M.TECH in Power system engineering from BVCITS Batlapalem Amalapuram, AICTE Engineering college Affiliated to JNTUK University, Kakinada in 2014 his field of interest include Power systems.

**Mail id: venkatanaresh204@gmail.com**



<sup>2</sup>**Sitaram Appari** was born in Amalapuram, E.G.Dt, on June 2, 1987. He received the B.Tech degree in Electrical & Electronics Engineering, from BVC COLLEGE of Engineering, Odalarevu in 2008. His M.Tech from University College of Engineering JNTUK Kakinada on Advanced Power Systems in 2012. He is currently an Assistant professor with BVC INSTITUTE OF TECHNOLOGY&SCIENCE, Amalapuram. His research interests include smart grids, power systems and multilevel converters.

**Mail id: sitaram235@gmail.com**